NJC

ROYAL SOCIETY OF CHEMISTRY

COMMUNICATION

View Article Online
View Journal | View Issue

Check for updates

Cite this: *New J. Chem.*, 2024, **48**, 19384

Received 22nd October 2024,
Accepted 31st October 2024

DOI: 10.1039/d4nj04586f

rsc.li/njc

Thermally activated sensitization of organics by lanthanide complexes for near-infrared photochemical upconversion†

Ling Zhang,[ac] Guohua Zhu,[ac] Rui Hu,[b] Guoqiang Yang,[bc] Jinping Chen,[a] Tianjun Yu,[a] Yi Li[ac] and Yi Zeng *[ac]

A series of solid-state triplet–triplet annihilation upconversion systems have been developed utilizing a penta-nuclear Yb complex as the sensitizer, converting near-infrared light into blue, green and red photons. The endothermic sensitization of organic annihilators by the Yb complex enables an anti-Stokes shift exceeding 1.3 eV.

The triplet–triplet annihilation upconversion (TTA-UC) process combines two triplet excitons to generate a higher energy singlet exciton in organic chromophores, allowing the conversion of lower energy photons into higher energy ones. It holds great application potential in various fields, including photocatalysis, photovoltaics, biological imaging and sensing, *etc.*[1–4] TTA-UC is usually achieved *via* a photosensitization strategy to accumulate enough triplet excitons for the annihilation process to occur.[5,6] Anti-Stokes shift, upconversion efficiency, excitation/emission spectral coverage, and excitation intensity threshold are among the key performance indicators in TTA-UC.[7] For upconversion systems, a significant anti-Stokes shift remains the most prominent and desirable metric, and ongoing efforts aim to achieve upconversion from near-infrared (NIR) to visible light.[8] Significant efforts have been made over the past decade to develop new sensitizers for TTA-UC with large anti-Stokes shifts, such as metal complexes, thermally activated delayed fluorescence chromophores, inorganic semiconductors and nanocrystals.[9–13] Recently, lanthanide complexes have garnered increasing attention as sensitizers in TTA-UC owing to their advantageous properties such as NIR absorption, the absence of intersystem crossing and minimal re-absorption effects.[14–16] Energy losses induced by intersystem crossing (ISC) in the conventional organic sensitizer such as porphyrin derivatives are mitigated by using the new sensitizers described above, and a greater energy gain during the upconversion has been achieved.[9–13] However, the downhill energy transfer during the sensitization process still loses some of the excitonic energy, limiting further expansion of the anti-Stokes shift (Fig. 1a). Schmidt *et al.* pioneered isoenergetic/slightly uphill energy transfer between the sensitizer and annihilator with the aid of entropy gain.[17] Our group and Durandin's group have demonstrated that a triplet energy-deficient sensitizer can effectively sensitize an annihilator in TTA-UC through thermally activated triplet energy transfer.[18,19] The endothermic triplet energy transfer from the sensitizer to the annihilator compensates for the energy loss during ISC and even gains additional energy, thereby extending the anti-Stokes shift of upconversion.

In our ongoing exploration of thermally activated sensitization of TTA-UC,[18,20–22] it is speculated that the incorporation of

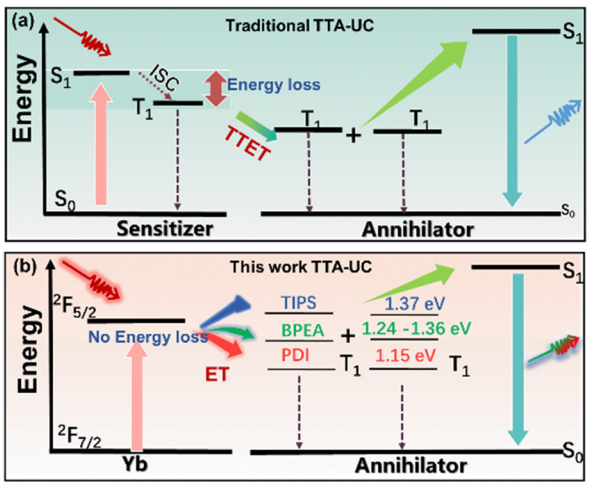

Fig. 1 Schematic energy diagram of traditional TTA-UC (a) and Yb-annihilator TTA-UC systems (b).

[a] *Key Laboratory of Photochemical Conversion and Optoelectronic Materials, Technical Institute of Physics and Chemistry, Chinese Academy of Sciences, Beijing 100190, China. E-mail: zengyi@mail.ipc.ac.cn*
[b] *Key Laboratory of Photochemistry, Institute of Chemistry, Chinese Academy of Sciences, Beijing 100190, China*
[c] *University of Chinese Academy of Sciences, Beijing 100049, China*

† Electronic supplementary information (ESI) available: Experimental and analytical data, Tables S1 and S2, and Fig. S1–S14. See DOI: https://doi.org/10.1039/d4nj04586f

lanthanide sensitizers and thermally activated sensitization would enable ultra-large anti-Stokes in TTA upconversion. Herein, three TTA-UC systems involving a penta-nuclear Yb complex as a sensitizer have been developed. The Yb complex can sensitize annihilators with different triplet energy levels, allowing these systems to achieve NIR upconversion and providing upconversion spectral coverage across the entire visible range (Fig. 1b). The Yb complex can sensitize aromatic annihilators *via* exothermic or endothermic triplet energy transfer, enabling TTA upconversion emission. Notably, the endothermic sensitization systems achieve anti-Stokes shifts of 1.16 and 1.32 eV, respectively. Lanthanide-activated upconversion luminescence can utilize the energy of more than two photons through cooperative energy transfer or cascade energy transfer processes, achieving large anti-Stokes shifts. Unlike TTA-UC in organic systems, rare-earth upconversion does not suffer from significant energy loss processes during intersystem crossing and energy transfer, resulting in significantly larger anti-Stokes shifts compared to TTA-UC. However, lanthanide upconversion materials typically exhibit narrow excitation and emission bands. Incorporating these materials with organic molecules can broaden the emission spectrum and enhance color diversity. Lanthanide complexes with NIR absorption can serve as a valuable complement to traditional TTA-UC materials, providing potential applications in sensing and three-dimensional displays. Moreover, thermally activated and conventional TTA-UC systems show an opposing trend toward temperature changes. Ratiometric luminescence temperature sensing has also been developed by combining TTA-UC materials of these two different sensitization mechanisms.

Yb complexes have emerged as promising sensitizer candidates due to the effective absorption in the NIR region compared with other lanthanide complexes. However, the utilization of Yb complexes in TTA-UC systems remains relatively limited.[16,23] In this work, the penta-nuclear $Yb_5(DBM)_{10}(OH)_5$ is chosen as the sensitizer due to its relatively large NIR absorption cross-section compared to other rare earth complexes, to study the TTA-UC of organic chromophores driven by it. $Yb_5(DBM)_{10}(OH)_5$ was prepared according to the previous report and the structure was characterized by single-crystal X-ray diffraction.[24,25] The Yb complex unit consists of a neutral cluster formed of five Yb atoms, ten dibenzoylmethane (DBM) ligands, and five hydroxyl groups. It is crystallized in tetragonal group $P4/n$, $Z = 2$ and the five Yb^{3+} ions are linked together through five hydrophilic hydroxo-bridges to give the $[Yb_5(OH)_5]^{10+}$ cluster core, presenting a regular square-based pyramidal geometry. Each Yb^{3+} ion is eight-coordinate. DBM ligands in $Yb_5(DBM)_{10}(OH)_5$ coordinated to the apical Yb atom are equiprobably disordered over two positions, which is associated with rotational distortion of the ligand. The absorption and luminescence spectra in dimethylformamide (DMF) and the structure of $Yb_5(DBM)_{10}(OH)_5$ are shown in Fig. 2a. The typical Yb core absorption peak is located at 980 nm with a molar absorption coefficient of 36 M^{-1} L^{-1}, making it a candidate for a NIR photosensitizer. Upon excitation with 980 nm NIR light, $Yb_5(DBM)_{10}(OH)_5$ emits luminescence with a peak at 1010 nm, which is attributed to the $^2F_{7/2} \rightarrow {}^2F_{5/2}$ transition. The NIR absorption and luminescence of $Yb_5(DBM)_{10}(OH)_5$ provide a transparent window and background-free condition for upconversion emission over a wide visible range.

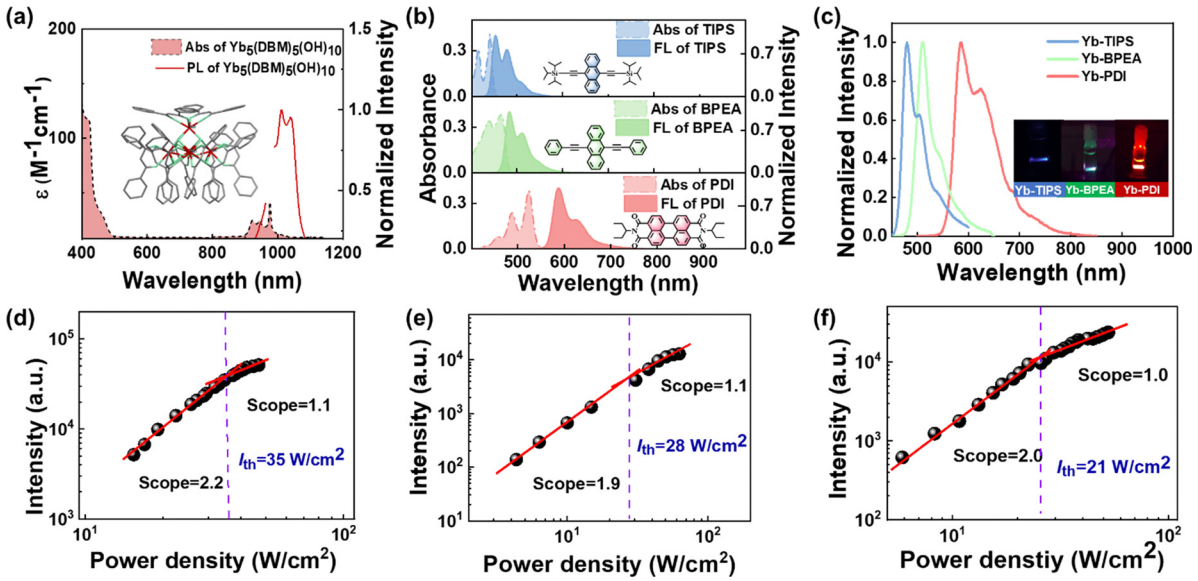

Fig. 2 (a) The absorption (dash line) and normalized photoluminescence (solid line) spectra of sensitizer $Yb_5(DBM)_{10}(OH)_5$ (λ_{ex} = 980 nm, 0.01 mol L^{-1}). (b) Absorption (dash-dot line) and normalized fluorescence (solid line) spectra of annihilators TIPS (blue shaded, λ_{ex} = 420 nm, 1.0 × 10^{-4} M), BPEA (green shaded, λ_{ex} = 430 nm, 1.0 × 10^{-4} M), and PDI (red shaded, λ_{ex} = 480 nm, 8.0 × 10^{-4} M) in DMF. Insets are the chemical structures of $Yb_5(DBM)_{10}(OH)_5$, TIPS, BPEA and PDI, respectively. UC emission spectra (c) of Yb–TIPS (2 : 1), Yb–BPEA (9 : 1), Yb–PDI (18 : 1) in DMF (λ_{ex} = 980 nm with a CW laser diode) and the insets are the corresponding photos of TTA-UC solution. Dependence of the TTA-UC intensity on the various incident power densities of (d) Yb–TIPS (6 : 1), (e) Yb–BPEA (9 : 1), and (f) Yb–PDI (36 : 1) (λ_{ex} = 980 nm). All UC tests were conducted by excitation by a 980 nm laser diode under an argon atmosphere.

Unlike conventional TTA-UC systems that rely on triplet–triplet energy transfer (TTET) from organic sensitizers and annihilators, lanthanide complexes capture lower-energy photons and directly deliver energy to the annihilator through an energy transfer (ET) process to avoid ISC energy loss (Fig. 1b). In addition, the energy difference between the Yb sensitizer and the annihilator triplet ($\Delta E = E_a - E_s$, where E_a and E_s are the energy levels of the annihilator triplet and the Yb sensitizer, respectively) plays a critical role in the ET process and further impacts the TTA-UC performance. TTA-UC systems of endothermic sensitization ($\Delta E > 0$) require thermal input from the environment to facilitate the ET process, thereby achieving additional energy gain. This ultimately results in larger anti-Stokes shifts and different temperature response compared to conventional TTA-UC systems ($\Delta E < 0$). To construct the exothermic and endothermic TTA-UC systems, three organic molecules, 9,10-bis((triisopropylsilyl)ethynyl)anthracene (TIPS), 9,10-bis(phenylethynyl) anthracene (BPEA), and *N*,*N*′-bis(ethylpropyl)perylene-3,4,9,10-tetracarboxylicdimide (PDI), were chosen as the annihilator based on their different triplet energy levels. The triplet energy level (1.24–1.36 eV) of BPEA[26,27] is equal to or slightly higher than the excitation energy of $Yb_5(DBM)_{10}(OH)_5$ (1.27 eV). The triplet energy levels of TIPS (1.37 eV)[8] and PDI (1.15 eV)[28,29] are significantly higher and lower than the excited energy level of the Yb complex. The absorption and luminescent spectra of the annihilators are shown in Fig. 2b. The TIPS, BPEA and PDI show emission peaks at 480, 510 and 610 nm, respectively. These emissions cover the visible range and fall just within the transparent window of the Yb complex absorption.

Each of the three annihilators is paired with $Yb_5(DBM)_{10}(OH)_5$ to construct the TTA-UC samples Yb–TIPS, Yb–BPEA and Yb–PDI, and Yb–PDI, respectively. Under 980 nm CW laser excitation, Yb–TIPS, Yb–BPEA and Yb–PDI exhibit distinct upconversion emission corresponding to the fluorescence of TIPS, BPEA and PDI, respectively (Fig. 2c). A record anti-Stokes shift of 1.32 eV was obtained in the Yb–TIPS system, based on the lowest absorption peak of the photosensitizer and the bluest emission peak of TIPS.[7] The anti-Stokes shift for Yb–BPEA and Yb–PDI was estimated to be 1.16 and 0.77 eV, respectively. The upconversion emission lifetimes (τ_{UC}) of Yb–TIPS, Yb–BPEA and Yb–PDI in DMF are in the microsecond range, which is three orders of magnitude longer than the corresponding fluorescence decay of the annihilator (Table 1), suggesting a delayed emission from TTA. The TTA-based upconversion mechanism is further supported by the excitation intensity dependence of the UC emission. Double-log plots of the UC emission *versus* excitation intensity of the Yb–TIPS, Yb–BPEA and Yb–PDI show a quadratic to linear transition, giving a threshold excitation intensity (I_{th}) (Fig. 2d–f). The excitation threshold of the UC material indicating the shift from the quadratic to the linear dependence regime is obtained in the order of twenty to thirty W cm^{-2}.

The energy transfer efficiency (η_{ET}) between the Yb cluster and the annihilator was further studied by time-resolved spectroscopy. Under excitation by a 980 nm pulse laser, the luminescence lifetime of $Yb_5(DBM)_{10}(OH)_5$ at 1010 nm is shortened while the annihilators are present. The η_{ET} from $Yb_5(DBM)_{10}(OH)_5$ to annihilators was estimated based on the equation: $\eta_{ET} = 1 - \tau_{Yb}/\tau_{Yb0}$, where τ_{Yb0} and τ_{Yb} are the luminescence lifetimes of the Yb complexes with and without annihilators in DMF, respectively. The η_{ET} of Yb–TIPS, Yb–BPEA and Yb–PDI is estimated to be 16.1, 22.2 and 13.2%, respectively (Table 1), indicating the occurrence of energy transfer from $Yb_5(DBM)_{10}(OH)_5$ to the annihilators. These results also confirm that the Yb complex can sensitize annihilators through endothermic energy transfer and then cause them to generate upconversion. Due to the high excitation threshold and high laser intensity, we were unable to measure reliable upconversion quantum efficiency for the present TTA-UC system.

Table 1 The photophysical parameters of TTA-UC and the emission lifetime of the sensitizer and annihilators in DMF

Sample	τ_{Yb} (μs)	η_{ET} (%)	I_{th} (W cm^{-2})	τ_{uc} (μs)	τ_{FL} (ns)
$Yb_5(DBM)_{10}(OH)_5$	8.7	—	—	—	—
Yb–TIPS (6 : 1)	7.3	16.1	35	8.9	4.8
Yb–BPEA (18 : 1)	7.0	22.2	28	6.8	3.8
Yb–PDI (18 : 1)	7.9	9.1	21	5.1	5.2

Solid-state samples with dense annihilators not only facilitate the triplet exciton diffusion in the annihilator matrix but also benefit the endothermic sensitization.[18,30] Therefore, the TTA-UC systems of Yb–TIPS, Yb–BPEA, and Yb–PDI were prepared into microcrystals by the co-precipitation method, respectively. Scanning electron microscopy (SEM) analysis reveals distinct morphologies among the three types of TTA-UC microcrystals (Fig. S6, ESI†). Yb–TIPS, Yb–BPEA, and Yb–PDI microcrystals exhibit polygonal, rod-like and leaf-like shapes, respectively. The powder X-ray diffraction (PXRD) of the TTA-UC microcrystals showed characteristic peaks from the sensitizer and the annihilator crystals (Fig. S7, ESI†). The energy transfer efficiencies from the sensitizer to the annihilators was increased in the microcrystals due to close packing of the components, and were estimated to be 31, 53 and 48% for Yb–TIPS, Yb–BPEA and Yb–PDI, respectively. The UC emission in the solid state is red-shifted compared to that in solution, resulting from molecular aggregation of the annihilator. We also measured I_{th} of the solid TTA-UC (Fig. S9, ESI†), which yielded values of 3.0, 2.5, and 2.3 W cm^{-2} for Yb–TIPS, Yb–BPEA, and Yb–PDI, respectively. The significantly lower I_{th} compared to that in solution is primarily due to more efficient energy transfer from the sensitizer to the annihilator in the solid state. The UC lifetimes for the three samples in the microcrystals exhibit distinct variation trends (Fig. S3, ESI†). Yb–TIPS microcrystals exhibit a slightly shorter upconversion lifetime (5.7 μs) compared to the solution, which may be attributed to the reduced fluorescence quantum efficiency and shortened lifetime in the solid state. In contrast, Yb–BPEA and Yb–PDI microcrystals show extended upconversion lifetimes, suggesting that the triplet excited states have longer lifetimes in the crystalline phase than those in the solution.

The effect of temperature on the TTA-UC was further studied since endothermic sensitization TTA-UC of Yb–TIPS, Yb–BPEA, and Yb–PDI at different temperatures has been investigated, respectively, and is shown in Fig. 3a, b and Fig. S10a (ESI†). The

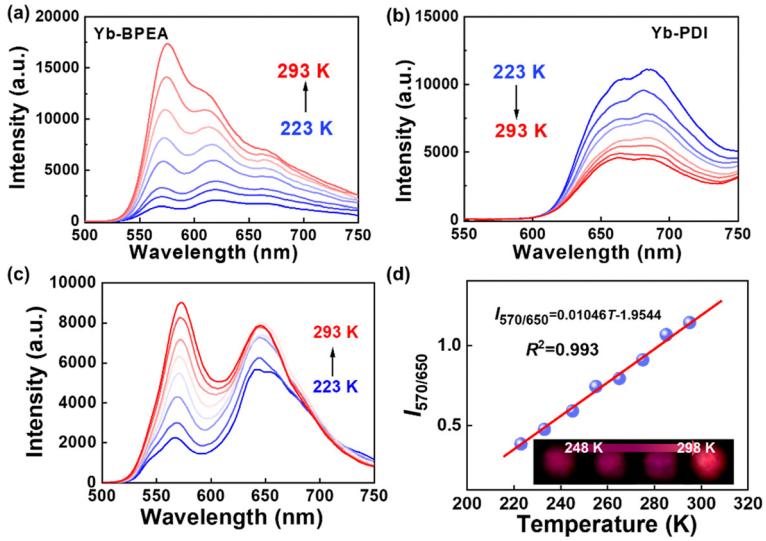

Fig. 3 Upconversion emission spectra of the Yb–BPEA microcrystals (molar ratio = 1 : 30) (a), the Yb–PDI microcrystals (molar ratio = 1 : 10) (b) and the mixed microcrystals of Yb–BPEA and Yb–PDI (mass ratio of Yb–BPEA/Yb–PDI is 1 : 4) (c) from 223 to 293 K upon excitation by a 980 nm CW laser diode. Intensity ratio ($I_{570/650}$) of Yb–BPEA/Yb–PDI (1 : 4) (d) obtained at various temperatures. Inset: upconversion images of the mixed microcrystals at various temperatures.

UC emission intensity of Yb–TIPS and Yb–BPEA increases as the temperature increases from 223 to 293 K, showing a different trend from that of Yb–PDI, a conventional TTA-UC system with exothermic sensitization. The upconversion enhancement with increasing temperature reflects the presence of a thermally activated energy transfer process in the TTA-UC system. Based on the triplet energy level of the annihilator and the excitonic energy of the Yb complex, it can be assumed that the annihilator in Yb–TIPS and Yb–BPEA is sensitized by Yb *via* a thermally activated energy transfer.

The contrasting temperature-dependent trends of TTA-UC emission make it possible to construct a ratiometric luminescent probe mixed with two TTA-UC microcrystals. Yb–BPEA and Yb–PDI microcrystals with stronger UC emission are selected because Yb–TIPS microcrystals have the weakest UC emission (Fig. S10b, ESI†). The mixed microcrystals with the mass ratio of Yb–BPEA to Yb–PDI of 1 : 4 shows dual emission peaks at 570 and 650 nm, corresponding to the upconversion emission peaks of Yb–BPEA and Yb–PDI microcrystals, respectively (Fig. 3c and Fig. S11, ESI†). Since Yb–BPEA with endothermic sensitization has an emission band around 650 nm, the enhancement of Yb–BPEA exceeds the attenuation of upconversion from Yb–PDI with exothermic sensitization as temperature increases. Consequently, the hybrid system exhibits an overall increase in upconversion with rising temperature, although the enhancement at longer wavelengths is weaker compared to that at shorter wavelengths. Plotting the intensity ratio ($I_{570/650}$) of the UC emission intensity at 570 and 650 nm against temperature changes from 223 to 293 K yields a good linear relationship, which can be described by $I_{570/650} = 1.05 \times 10^{-2}T$-1.95 with a fitting correlation coefficient (R^2) value of 0.993 (Fig. 3d). While the temperature increases, the change of luminescent color from plum to reddish-orange can be observed without filters (Fig. 3d). The maximum relative thermal sensitivity (Sr) was determined to be 2.71%/K (Fig. S12, ESI†). The chemical composition of the mixed TTA-UC microcrystals of (Yb–BPEA/Yb–PDI) was tested using energy dispersive X-ray spectroscopy (EDX), as shown in Fig. S13 and S14 (ESI†). The EDX spectrum of the mixed microcrystals shows the uniform distribution of all four elements at the current resolution, indicating no obviously segregation in the doped microcrystals.

In summary, we have incorporated $Yb_5(DBM)_{10}(OH)_5$ as a NIR sensitizer and three organic annihilators with different triplet energy levels to achieve TTA-UC from NIR to blue, green and red photons in the solid state. The Yb complex sensitizes the annihilator *via* exothermic or endothermic triplet energy transfer and a record anti-Stokes shift of 1.32 eV is obtained in a thermally activated sensitization combination (Yb–TIPS). Based on the opposing temperature responsiveness of the UC emission intensity from exothermic and endothermic sensitized TTA-UC, a ratiometric luminescent temperature sensing material has been developed by combining these two TTA-UC materials. Although the upconversion emission in the blue region was too weak to achieve a white-light TTA-UC combination, lanthanide complexes still demonstrate significant potential in NIR photochemical upconversion. The utilization of lanthanide complexes to sensitize organic annihilators is emerging due to the potential for achieving large anti-Stokes shifts, moderate excitation intensities, and diverse upconversion spectra, despite some inherent shortcomings such as low absorption cross-sections in lanthanide complexes.

We are grateful for the financial support from the National Natural Science Foundation of China (22273117, 22273110 and 22090012).

Data availability

The data supporting this article have been included as part of the ESI.†

Conflicts of interest

There are no conflicts to declare.

References

1 T. F. Schulze and T. W. Schmidt, *Energy Environ. Sci.*, 2015, **8**, 103–125.
2 B. S. Richards, D. Hudry, D. Busko, A. Turshatov and I. A. Howard, *Chem. Rev.*, 2021, **121**, 9165–9195.
3 S. E. Seo, H. S. Choe, H. Cho, H. I. Kim, J. H. Kim and O. S. Kwon, *J. Mater. Chem. C*, 2022, **10**, 4483–4496.
4 L. Huang and G. Han, *Nat. Rev. Chem.*, 2024, **8**, 238–255.
5 T. N. Singh-Rachford and F. N. Castellano, *Coord. Chem. Rev.*, 2010, **254**, 2560–2573.
6 J. Zhou, Q. Liu, W. Feng, Y. Sun and F. Y. Li, *Chem. Rev.*, 2015, **115**, 395–465.
7 Y. Zhou, F. N. Castellano, T. W. Schmidt and K. Hanson, *ACS Energy Lett.*, 2020, **5**, 2322–2326.
8 P. Bharmoria, H. Bildirir and K. Moth-Poulsen, *Chem. Soc. Rev.*, 2020, **49**, 6529–6554.
9 N. Yanai and N. Kimizuka, *Acc. Chem. Res.*, 2017, **50**, 2487–2495.
10 Z. H. Xu, Z. Y. Huang, T. Jin, T. Q. Lian and M. L. Tang, *Acc. Chem. Res.*, 2021, **54**, 70–80.
11 Y. Y. Han, S. He and K. F. Wu, *ACS Energy Lett.*, 2021, **6**, 3151–3166.
12 C. M. Sullivan and L. Nienhaus, *Nanoscale*, 2023, **15**, 998–1013.
13 K. Ye, M. Imran, X. Chen and J. Zhao, *ACS Appl. Opt. Mater.*, 2024, **2**, 1803–1824.
14 S. H. Wen, J. J. Zhou, P. J. Schuck, Y. D. Suh, T. W. Schmidt and D. Y. Jin, *Nat. Photonics*, 2019, **13**, 828–838.
15 G. C. Bao, R. R. Deng, D. Y. Jin and X. G. Liu, *Nat. Rev. Mater.*, 2024, DOI: **10.1038/s41578-024-00704-y**.
16 N. Kiseleva, P. Nazari, C. Dee, D. Busko, B. S. Richards, M. Seitz, I. A. Howard and A. Turshatov, *J. Phys. Chem. Lett.*, 2020, **11**, 2477–2481.
17 Y. Y. Cheng, B. Fuckel, T. Khoury, R. G. C. R. Clady, N. J. Ekins-Daukes, M. J. Crossley and T. W. Schmidt, *J. Phys. Chem. A*, 2011, **115**, 1047–1053.
18 L. Li, Y. Zeng, J. P. Chen, T. J. Yu, R. Hu, G. Q. Yang and Y. Li, *J. Phys. Chem. Lett.*, 2019, **10**, 6239–6245.
19 J. Isokuortti, S. R. Allu, A. Efimov, E. Vuorimaa-Laukkanen, N. V. Tkachenko, S. A. Vinogradov, T. Laaksonen and N. A. Durandin, *J. Phys. Chem. Lett.*, 2020, **11**, 318–324.
20 W. X. Yin, T. J. Yu, J. P. Chen, R. Hu, G. Q. Yang, Y. Zeng and Y. Li, *ACS Appl. Mater. Interfaces*, 2021, **13**, 57481–57488.
21 G. W. Luo, Y. P. Liu, Y. Zeng, T. J. Yu, J. P. Chen, R. Hu, G. Q. Yang and Y. Li, *J. Mater. Chem. C*, 2022, **10**, 8596–8601.
22 P. F. Niu, X. Da, R. Hu, T. J. Yu, J. P. Chen, Q. X. Zhou, G. W. Luo, Y. Zeng and Y. Li, *New J. Chem.*, 2024, **48**, 6886–6892.
23 S. Han, R. Deng, Q. Gu, L. Ni, U. Huynh, J. Zhang, Z. Yi, B. Zhao, H. Tamura, A. Pershin, H. Xu, Z. Huang, S. Ahmad, M. Abdi-Jalebi, A. Sadhanala, M. L. Tang, A. Bakulin, D. Beljonne, X. Liu and A. Rao, *Nature*, 2020, **587**, 594–599.
24 H. Y. Shen, W. M. Wang, H. L. Gao and J. Z. Cui, *RSC Adv.*, 2016, **6**, 34165–34174.
25 T. S. Sukhikh, D. A. Bashirov, N. V. Kuratieva, A. I. Smolentsev and S. N. Konchenko, *J. Struct. Chem.*, 2014, **55**, 1437–1441.
26 Y. J. Bae, G. Kang, C. D. Malliakas, J. N. Nelson, J. Zhou, R. M. Young, Y. L. Wu, R. P. Van Duyne, G. C. Schatz and M. R. Wasielewski, *J. Am. Chem. Soc.*, 2018, **140**, 15140–15144.
27 Y. Niihori, T. Kosaka and Y. Negishi, *Mater. Horiz.*, 2024, **11**, 2304–2322.
28 P. Jack Ka Hei, K. G. Joseph, F. Laszlo, K. K. P. Shyamal, B. D. Cameron, W. M. Rowan and W. S. Timothy, *J. Photonics Energy*, 2018, **8**, 022006.
29 F. Deng, J. R. Sommer, M. Myahkostupov, K. S. Schanze and F. N. Castellano, *Chem. Commun.*, 2013, **49**, 7406–7408.
30 B. Joarder, N. Yanai and N. Kimizuka, *J. Phys. Chem. Lett.*, 2018, **9**, 4613–4624.

